XVII IAHR SYMPOSIUM
Beijing, China 1994

UNSTABLE PART-LOAD OPERATION OF A MODEL FRANCIS TURBINE: EVALUATION OF DISTURBANCE MAGNITUDE

Thierry Jacob and Jean-Eustache Prénat, IMHEF - EPF Lausanne
Switzerland
Giuseppe Angelico, ENEL SPA - DSR - CRIS Milano
Italy

ABSTRACT

The low frequency pressure oscillations observed at the draft tube wall of a Francis turbine operating at part load may be split into two uniform components: a rotating pressure with a constant area-averaged value, and a synchronous pulse involving the whole draft tube section.

The synchronous pulse is sometimes used to evaluate the magnitude of disturbances generated by part-load operation of the turbine. A more global way to evaluate the magnitude of these disturbances is to estimate the emission of acoustic power at the spiral case inlet.

In this paper, both methods are used on model test data from a high specific speed turbine. A good correlation is found between results from the two approaches.

RESUME

Les oscillations de pression à basse fréquence observées en paroi du cône de l'aspirateur des turbines Francis fonctionnant à débit réduit peuvent être divisées en deux composantes uniformes: une pression tournante dont la valeur moyenne sur une section est constante, et une pulsation synchrone sur toute la section de l'aspirateur.

On utilise parfois la pulsation synchrone pour évaluer l'intensité des perturbations générées par le fonctionnement de la turbine à débit partiel. Une approche plus globale passe par l'estimation des émissions de puissance acoustique à l'entrée de la bâche spirale.

Les deux méthodes sont appliquées dans cet article à des résultats d'essais sur modèle réduit d'une turbine de vitesse spécifique élevée. On trouve une bonne corrélation entre les résultats obtenus avec ces différentes approches.

Le texte en français peut être obtenu auprès des auteurs.

G12

0. Introduction

Part load instability of Francis turbines is a well known phenomenon that must always be considered at design stage. Excessive responses to this disturbance sometimes impose restrictions on the operation of important hydro-electric plants.

The instability is due to the interaction of the runner outlet swirl with the draft tube diverging cone and elbow. The swirling flow in the draft tube cone organizes into a precession movement: the vortex is not centered but slowly rotates, typically between one quarter and one third of runner rotational frequency. Rotating fields of flow velocity and pressure are associated with the precession movement.

For a given draft tube geometry, the basic parameter for draft tube flow precession is the swirl momentum parameter, a cross-sectional area averaged function of axial and peripheral velocities [8]. Global approaches involving a swirl parameter estimated from the operating conditions and efficiency characteristic, however, are not sufficient because of the decisive influence of small differences in the distribution of axial and peripheral velocities [4].

The precession does not circle around the draft tube center-line. Depending mostly on the existence and design of a draft tube bend, it is shifted toward the wall. This means that the cross-sectional area averaged instantaneous pressure varies with time. In this way, the precession acts as a fluctuating pressure source concentrated below the runner.

Under the joint action of high peripheral velocities and low pressure levels at the runner outlet, a large vapor-filled cavity forms along the vortex center-line. Its rotation with the precession results in the well-known helical draft tube vortex. The water plug in the draft tube oscillates against the elastic vapor volume of draft tube cavitation. The frequency of these free oscillations is often in the same range as the precession frequency. When they become close or equal, draft tube resonance occurs. This generates an important excitation to the penstock and to the rotating machinery [4].

It is not so easy to measure the magnitude of the excitation associated with the part-load precession. Direct measurements of draft tube wall pressure are clearly insufficient, as the pressure oscillation amplitude varies along the periphery. An evaluation based on the amplitudes and phase shifts of pressure oscillations from several positions around the draft tube provides a better view of what happens [5, 6]. Combined in the time or frequency domain, the pressure signals associated with the precession may be split into a rotating and a synchronous (pulsating) component [1, 7, 8, 9]. The rotating component is purely neutral from the point of view of system excitation. The synchronous component may then be understood as a pressure source representing the disturbance. The problem, then, is that the estimated synchronous component of the precession may be influenced by standing waves from the upstream piping [1].

One way to separate the emission of oscillatory energy (travelling waves) from the standing waves is to evaluate the acoustic power at the spiral case inlet [4]. This measurement is basically simple, but some difficulties may arise from its actual use.

In the following pages, we will proceed from general observations of part load stability of operation on a Francis turbine model to estimate the rotating and synchronous components of the precession. They will then be compared with a source pressure derived from measurements of acoustic power in the feed pipe.

1. Model test arrangement and basic results

The purpose of the model tests presented in this paper is a better understanding of the unstable part-load operation of the turbines at Pescara 1° Salto. This plant is equipped with two small Francis turbines, 1.91 m in runner outlet diameter, rated power 5.8 MW each, commissioned in 1947.

A project to automate the operation of the plant stimulated studies to solve the problem of part-load instability for these turbines. Field measurements were conducted by ENEL [2, 3]. A scale model with a 0.400 m runner outlet diameter was built under contract from ENEL and is now experimented at IMHEF. The analysis presented in this paper was performed as a part of this test program.

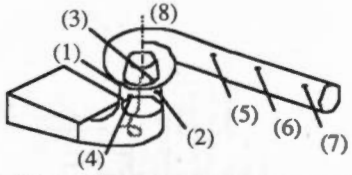

figure 1: Model test arrangement with measurement channels

As shown on figure 1, pressure fluctuations are measured at four positions (1, 2, 3, 4) in a transverse section of the draft tube cone. Three more pressure sensors (5, 6, 7) are equally spaced on the feed pipe. Shaft torque oscillations (8) are also measured. The signals are digitally processed [5] in the frequency domain with a multi-channel FFT analyzer.
Operating conditions are specified by relative flow and energy coefficients. With Q as the volume flow-rate, R the runner blade outlet outer radius, ω the runner angular speed and E the specific hydraulic energy, these parameters are:

$$\text{flow coefficient: } \varphi = \frac{Q}{\pi R^3 \omega} \quad ; \quad \text{energy coefficient: } \psi = \frac{2E}{R^2\omega^2}$$

Flow and energy coefficients are normalized by their values at best efficiency. The specific speed is specially high for a Francis turbine: $\nu_{ref} = \varphi_{ref}^{1/2} \cdot \psi_{ref}^{-3/4} = 0.675$.
To ensure similitude of draft tube cavitation, the reference elevation for Thoma number σ is set at the runner outlet periphery: $\sigma = \sigma_{1e}$.
The discussions in this paper are focused on the operation at 78.8 % of best efficiency energy coefficient ψ_{ref}. The draft tube pressure level is low: $\sigma_{1e} = 0.327$. The specific hydraulic energy selected for the tests is E = 146.9 J/kg. The model runner rotational frequency is n = 17.6 Hz.
Amplitude spectra of pressure oscillations at the downstream side of cone (position 1, figure 1) are plotted versus flow coefficient on the waterfall diagram of figure 2. Frequencies are normalized by the rotational frequency. Amplitudes are normalized by the test head pressure.
Significant frequencies are sorted from the FFT data on the basis of amplitude, phase shift and coherence criteria and represented on the synoptic diagram of figure 3. In its upper portion, the synoptic diagram [6] shows the evolution versus flow coefficient of the precession frequency (o), its second harmonic (●) and the draft tube free oscillations frequency (o´), all normalized by the runner rotational frequency. Associated pressure oscillation amplitudes at the downstream side of cone are plotted using triangles with the same styles. Amplitudes are root mean square and normalized by the test head.
The triangles in the middle portion show the amplitude of pressure oscillations at the upstream side of cone. The squares show the phase shift, at the precession frequency, of upstream side to downstream side of cone. The triangles in the lower portion show the pressure oscillation amplitudes at the spiral case inlet. The squares show the torque oscillation amplitude at the precession frequency. Torque oscillation amplitudes are normalized by the best efficiency torque at the considered test head.
At very low flows, the runner outlet swirl is high but axial velocities are small. There is no organized precession.
Starting at $\varphi/\varphi_{ref} = 0.64$, the part load instability develops with a dominant sine oscillation close to f/n = 0.25 and a small second harmonic. The amplitude of the pressure oscillation associated with the precession is close to 4 % RMS of the test head at the downstream side of cone. It is much lower on the upstream side of cone and at the spiral case inlet. At the precession frequency, torque and spiral case inlet pressure oscillation amplitudes follow the same evolution.
Draft tube free oscillations (o´, Δ´) occur between 0.35 • n and 0.9 • n. The frequency is lowest when the draft tube cavity volume is greatest, between 0.72 φ_{ref} and 0.75 φ_{ref}. It is then close to the precession frequency. Higher amplitudes in this range of flow show that the free oscillations are excited by side bands of the precession. Also, side bands of the free oscillations influence the precession: at 0.725 φ_{ref}, the difference in amplitude between downstream and

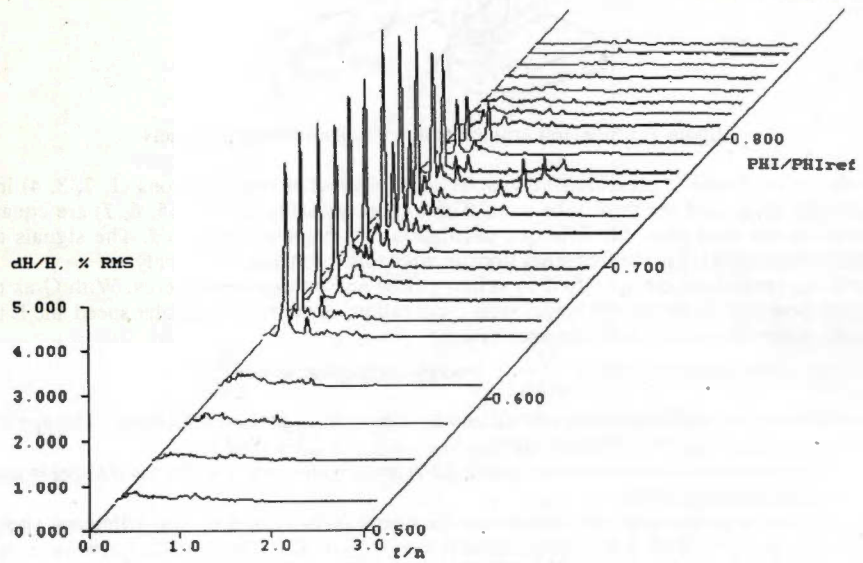

figure 2: Waterfall diagram of pressure oscillation amplitudes on the downstream side of draft tube wall, operation at 0.788 ψ_{ref}, σ_{1e} = 0.327, E = 146.9 J/kg

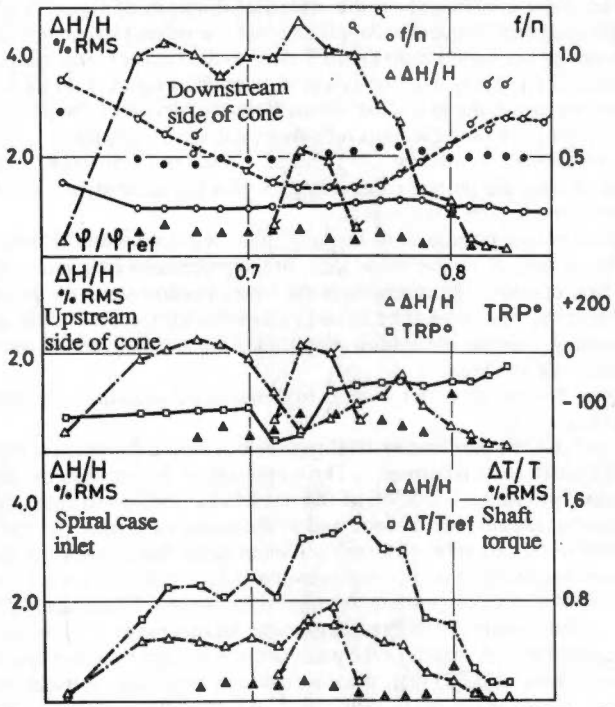

figure 3: Synoptic diagram for operation at 0.788 ψ_{ref}, σ_{1e} = 0.327, E = 146.9 J/kg

upstream side of cone is a remarkable 4.65 % to 0.4 % RMS of the test head.
The high partial load oscillation [4] stands out as a group of peaks just above the rotational frequency at 0.75 φ_{ref} on the waterfall diagram.
The explored range of flow lies below the vortex-free region. There are no full-load pulsations. Inter-blade cavitation tails (crown-attached or blade inlet vortices) are visible below 0.67 φ_{ref}. The part-load helical vortex is visualized by loose bubbles starting at 0.57 φ_{ref} and has a compact vapor core for $0.69 \leq \varphi/\varphi_{ref} \leq 0.80$. A pounding sound is generated at 0.76 φ_{ref}. A thin, unstable helical vortex cavity is observed at 0.84 φ_{ref}. An axially centered cavity develops above 0.85 φ_{ref} with blade outlet cavitation.

2. Estimation of the draft tube pressure source

The pressure oscillation is collected from several sensors on the draft tube periphery. Rotating and synchronous components of the precession may be extracted in the time or frequency domain.
Time domain processing [8, 9] involves the averaging of whole time records, with acquisition triggered by the oscillation at the reference channel. This will give correct results only if the oscillation is very periodic. If secondary frequencies generate a beat (as the draft tube free oscillations do at 0.72 φ_{ref} in the example of figure 2), or if bursts of higher frequency oscillations (such as the high partial load) occur, time averaging is not appropriate.
Figure 4 shows the assembly in the complex plane [1, 7] of vectors representing the Fourier transformed pressure oscillations from the draft tube cone periphery at the precession frequency. The construction to estimate the rotating and synchronous components of the precession is illustrated in figure 4 (a, b, c) for an investigation using two, three and more than three pressure sensors respectively.

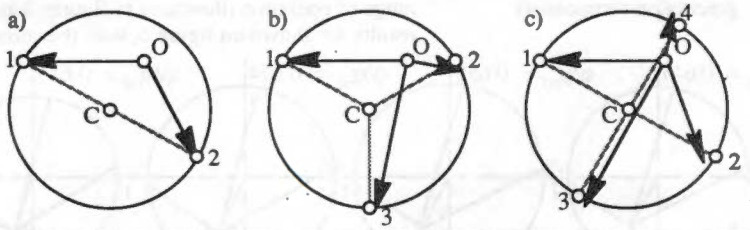

figure 4: Vectorial assembly of pressure oscillations in a draft tube cone transverse section

a) Two pressure sensors are placed on either side of the draft tube cone diameter. The associated vectors are plotted from the origin (O). They theoretically point to the angular positions of the sensors (1), (2) on the draft tube cone wall. This determines the center of rotation (C). The synchronous component of the precession is the distance (OC). The rotating component is the circle radius. With a little bit more complication, this construction may also be done with angular positions of the sensors other than 180°.
b) Three pressure sensors are placed around the periphery of a transverse section of the draft tube cone. The associated vectors are plotted from the origin (O). They theoretically point to the angular positions of the sensors. The three vectors define a circle centered in (C). The synchronous component of the precession is the distance (OC). The rotating component is the circle radius. Due to measurement errors, the angular positions of the pressure vectors will not perfectly coincide with the geometrical positions of the sensors. This gives us an idea of the precision of the method.
c) More than three pressure sensors are placed around the draft tube cone periphery. The procedure is run as in b), except that the circle is now a best fit from the data points. Due to measurement errors, not only the angular positions but also the distance to (C) of the pressure vectors will not perfectly coincide with the geometrical positions of the sensors on the circle. This gives us a better idea of the precision of the method.

Misleading results may come out of this processing if it is inappropriately used on pressure oscillations which cannot be split into a rotation and a pulsation. A typical example of this is the second harmonic of the precession frequency. For oscillations of such nature, there is no direct relation between the angular positions of pressure vectors and associated sensors.
Some turbines have non-circular draft tube cone cross-sections. It is then uncomfortable to define a purely rotating component of the precession although the problem is not fundamentally different from the circular cross-section. As these draft tube designs are known for the intense excitation they sometimes generate at part load, special investigations should be run on this particular problem.

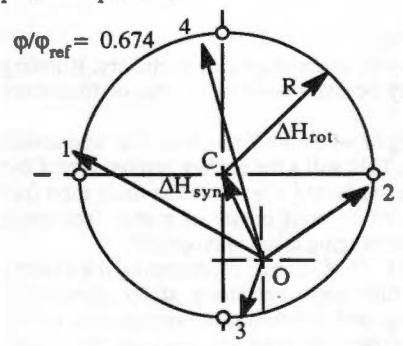

figure 5: Rotating and synchronous precession components

Once the circle defining the rotating and synchronous components of the precession is determined, the whole figure is rotated in order for the angular positions of the pressure vectors to fit best with the geometrical position of the sensors. This is shown in figure 5.
Point O, from which the pressure vectors originate, should not be understood as the center of rotation of the precession movement. This center is somewhere in the opposite portion of the draft tube cross-section. Anyhow, the precession has few chances of actually being circular.
The splitting of the precession oscillation into rotating and synchronous components was performed with variable flow coefficient, in the range of operation illustrated in figures 2 and 3. The results are shown on figure 6, with the downstream

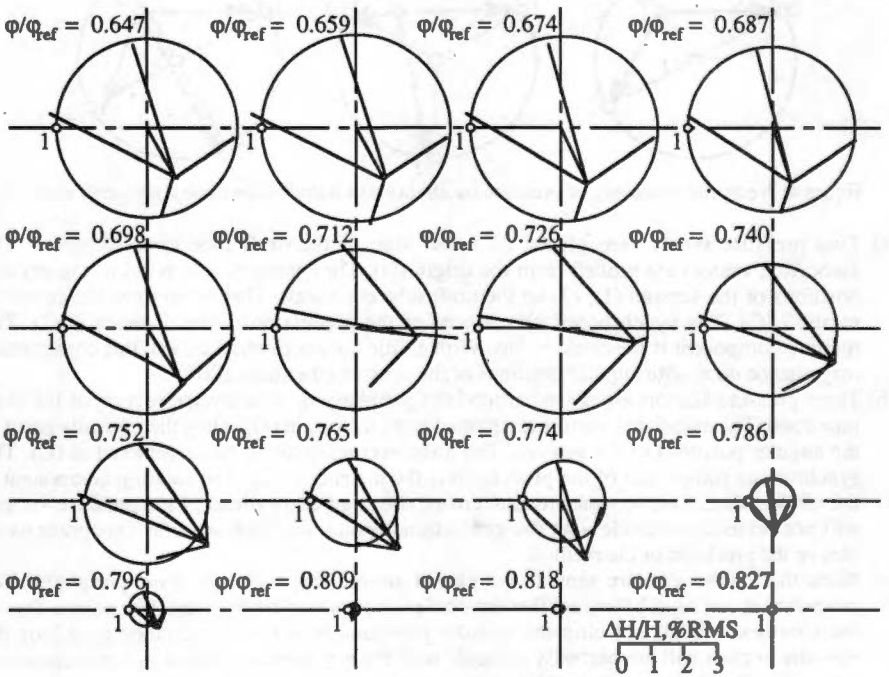

figure 6: Vectorial assembly with variable flow coefficient at 0.788 ψ_{ref}, σ_{1e} = 0.327

side of cone on the left. The construction at 0.726 φ_{ref} is specially interesting. It shows how the pressure vectors compose at this point where side-bands of the draft tube free oscillations influence the precession. The amplitude at the upstream side of cone drops sharply, but the rotating pressure fluctuation is not smaller than for the neighboring flow coefficients.
Starting at 0.740 φ_{ref}, the rotating component of the precession decays. The synchronous component dominates, then dies down above 0.82 φ_{ref}. Even when amplitudes are very small, the pressure vectors agree well with the sensor positions.
Marginally, the constructions in figure 6 systematically feature the same shift between angular positions of the pressure vectors and associated sensors. Vectors 1 and 2 are rotated clockwise from the sensors, vectors 3 and 4 are rotated counterclockwise.
From this graphical display of test results, we can say that an estimation of the synchronous component of the precession based on pressure data from the downstream and upstream sides of cone only (left and right on the plots) would already have given fairly good results in this case.

3. Draft tube pressure source and acoustic power emission

The synchronous component of the part load precession is easily estimated from the pressure signals from sensors placed around a transverse section of the draft tube cone. It represents the pressure source associated with the part load disturbance.
How is this pressure source influenced by standing waves in the test circuit? How does it propagate through the runner and spiral case? To answer these questions, we compared the draft tube pressure source with the acoustic power emission at the spiral case inlet.
The global acoustic power GAP [4] is the active part of the power associated with the hydro-acoustic oscillation. Its estimation from pressure signals collected at different locations along the feed pipe is straightforward and easily automated. This processing eliminates the influence of standing waves in the feed pipe. The acoustic power multiplied by the reference acoustic impedance is a squared pressure source. Normalized by the test head pressure, it is a transposable test result [6].

$$\frac{\Delta H_{src}}{H} = \frac{1}{\rho E}\sqrt{GAP \cdot Z_0}$$

The pressure source ΔH_{src} from the acoustic power measurement at the spiral case inlet is compared with the rotating and synchronous components ΔH_{rot} and ΔH_{syn} of the precession oscillation. This is done for the range of operating conditions investigated in the previous sections. Figure 7 shows ΔH_{rot}, ΔH_{syn} and ΔH_{src} versus flow coefficient φ.
The rotating pulse ΔH_{rot} decays almost steadily over this variation of flow coefficient. The synchronous pulse is maximum for $0.725 \le \varphi/\varphi_{ref} \le 0.75$, where the precession is influenced

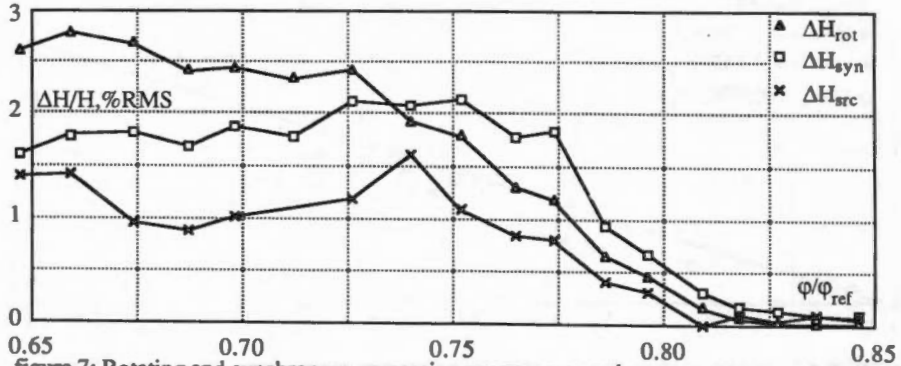

figure 7: Rotating and synchronous precession components and source pressure at the spiral case inlet for operation at 0.788 ψ_{ref}, σ_{ie} = 0.327, E = 146.9 J/kg

by side-bands of the draft tube free oscillations. Above 0.75 φ_{ref}, it dies down but still dominates ΔH_{rot}, as we already saw from figure 6. The pressure source ΔH_{src} at the spiral case inlet follows the same overall evolution as the synchronous pulse ΔH_{syn}, except below 0.67 φ_{ref}. Results of the same nature were obtained for tests with different values of energy coefficient ψ and Thoma number σ.

The resemblance between the evolutions of ΔH_{syn} and ΔH_{src} suggests a strong correlation between these two pressure source magnitudes. To make this clear, ΔH_{src} was plotted versus ΔH_{syn} in figure 8. Two other test series were added on this diagram.

A linear best fit was run on this data, yielding a gain factor and a correlation coefficient.

The correlation is fairly good: 96%. The transmission of acoustic disturbances through the runner and spiral case of a Francis turbine was shown to be linear [4], so this good correlation mainly suggests that the estimated synchronous pulses were not much affected by superimposed standing waves in the test circuit. This is true in this series of tests, but will not always be the case.

The transmission could be expected to change according to frequency. As may be seen in figure 3, the precession frequency undergoes small variations. More directly, the runner rotational frequency varies by 17% between best efficiency ψ (blank squares in figure 8) and 0.757 ψ_{ref} (black triangles). The correlation was not improved by sorting the data by frequencies.

The transmission could also be expected to change according to flow coefficient. One reason is the variation in the head-flow characteristic which dominates in the real impedance of the turbine. Another reason is the variation in guide vane channel length and width, which modifies the inertance of water passages between runner and spiral case. No such influence, however, comes out clearly from the ΔH_{src} and ΔH_{syn} curves plotted versus flow coefficient in figure 7. The same plots for the two other energy coefficients in figure 8 do not clearly suggest such an influence either.

The gain factor between the pressure sources in the draft tube cone and at the spiral case inlet was found to be 0.6623. As the source of disturbances associated with the precession is obviously located in the draft tube and as the runner may be expected to provide some damping, it is satisfying to find a gain factor smaller than one. Not much more can be said at this level of our investigations. The application of the method should be improved in order to reduce the scatter.

If a more detailed insight on this gain factor is desirable, the investigation should start with some interesting questions on the generation and transmission of the synchronous pulsation associated with the part load precession.

What are the dynamic influences of boundary conditions, both hydraulic and mechanical? Model tests with different feed pipe configurations showed an important effect on the amplitude of part load oscillations. We may also imagine that, according to the generator dynamic

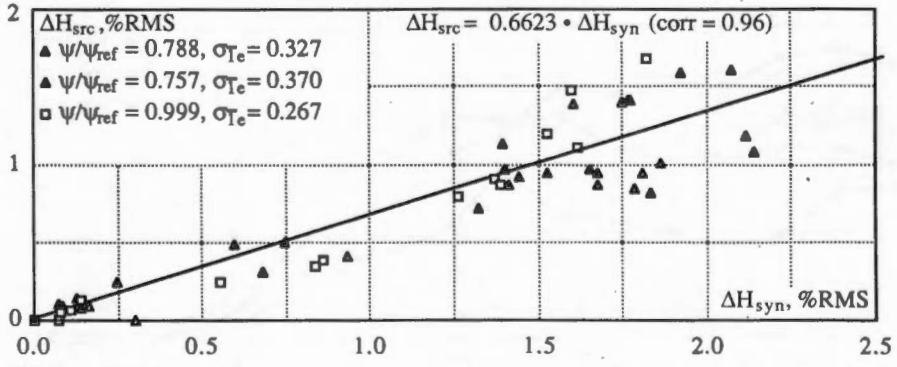

figure 8: Correlation of synchronous precession component and source pressure at spiral case inlet for various part load operating conditions

behavior, some oscillatory power may be exchanged with the rotating masses and electrical circuit [1].
How is the splitting of the precession into rotating and synchronous components influenced by the position of the measurement section along the height of the draft tube cone? If there are variations, how are they affected by draft tube cavitation?
How is the gain factor influenced by mechanical details of the model construction? This question covers both the stiffness of the spiral case and possible damping due to seal movements.
The scope of these questions is not limited to the particular topic of splitting precession oscillations. It extends to the general study of the transposition of stability of operation from model test results.
The method presented in this paper is valid only for oscillations which originate from uniform rotating and synchronous components within the considered circular cross-section of the draft tube cone. In this respect, the evaluation of acoustic power emission at the spiral case inlet has a much wider field of application. In fact, the good correlation found between the pressure sources associated with the synchronous component of the precession in the draft tube and with the acoustic power emission at the spiral case inlet is rather a validation of acoustic power analysis than a new perspective for splitting the precession.

5. Conclusions

Pressure oscillations associated with the part load precession, measured on a model Francis turbine, were separated into uniform rotating and synchronous components. This processing was done with good results over a wide range of flows.
The synchronous component of the precession may be imagined as a pressure source representing the disturbance imposed on the system. It was compared with the source pressure extracted from an estimation of acoustic power emission at the spiral case inlet. The comparison showed a good correlation.
To give a physical meaning to the gain factor between the source pressure at the spiral case inlet and the synchronous component of the precession, some parameters should be explored experimentally. Among these are:

- the influence of feed pipe and rotating masses boundary conditions;
- the influence of measurement section elevation within the draft tube cone;
- the influence of model construction stiffness.

Based on the presented model test results, a good agreement was found between estimations of the part load disturbance magnitude through acoustic power analysis and through the vectorial construction of pressure oscillations in the draft tube cone circumference.

Symbols

A	Cross-sectional area	m^2
E	Specific hydraulic energy	J/kg
GAP	Global acoustic power	W
n	Rotational frequency ($n = \omega/2\pi$)	Hz
q	Frequency volume flow-rate	m^3/s
R	Runner reference radius (at $_{le}$)	m
t	Time	s
φ	Flow coefficient	
Δ	Difference, variation, amplitude	
ρ	Mass per unit volume	kg/m^3
$_0$	(subscript) Reference	
$_{le}$	(subscript) Runner blade outlet periphery	
$_{src}$	(subscript) Source at spiral case inlet	
C	Reference or flow velocity	m/s
f	Frequency	Hz
H	Head (height of liquid column)	m
p	Pressure	N/m^2
Q	Time volume flow-rate	m^3/s
S	Wave propagation speed	m/s
Z_0	Reference impedance $\Delta p/\Delta Q$	$kg\ m^{-4}\ s^{-1}$
ψ	Energy coefficient	
σ	Thoma number	
ω	Runner angular speed	rad/s
$_{ref}$	(subsrcipt) At best efficiency operation	
$_{rot}$	(subscript) Rotating	
$_{syn}$	(subscript) Synchronous	

References

[1] ANGELICO G., MUCIACCIA F., ROSSI G.: Part load behaviour of a turbine: a study on a complete model of a hydraulic power plant. IAHR Symposium, Montréal (1986)

[2] ENEL DPT: Centrale idroelettrica Pescara 1° Salto: Rilievi sul comportamento del macchinario idraulico in condizioni oscillanti stazionarie. Roma (1990)

[3] GIACANELLI E., MASINI G., SELLO S., VANZAN R.: Non-linear oscillatory phenomena induced by hydraulic machinery: setting up of a digital data base and data analysis relevant to the Pescara Hydroelectric power plant. IAHR WG, Milano (1991)

[4] JACOB T.: Evaluation sur modèle réduit et prédiction de la stabilité de fonctionnement des turbines Francis. Thèse EPFL N° 1146, Lausanne (1993)

[5] JACOB T., PRENAT J.E.: TOME E.: Model testing for the stability of operation of Francis turbines. MTM Conference, Budapest (1994)

[6] JACOB T. PRENAT J.E.: Evaluation from model tests for a prediction of the stability of operation of Francis turbines. IAHR Symposium, Beijing (1994)

[7] MUCIACCIA F., ROSSI G.: Experimental approach to the study of the dynamic behavior of a Francis turbine model at high specific speed when operating at reduced load: splitting of the pressure pulsation below the runner at rope frequency into rotating and stationary component. IAHR WG, Mexico (1985)

[8] NISHI M., MATSUNAGA S., OKAMOTO M., TAKATSU K.: Wall pressure measurements as a diagnosis of draft tube surge. IAHR Symposium, Belgrade (1990)

[9] NISHI M.: Pressure data analysis by using Nishi's method. Kyushu Institute of Technology (1992)